J. Biochem. 128, 965–974 (2000)

X-Ray Crystal Structure and Catalytic Properties of Thr252Ile Mutant of Cytochrome P450cam: Roles of Thr252 and Water in the Active Center[1]

Takako Hishiki,* Hideo Shimada,* Shingo Nagano,* Tsuyoshi Egawa,* Yasukazu Kanamori,*[2] Ryu Makino,*[3] Sam-Yong Park,† Shin-ichi Adachi,† Yoshitsugu Shiro,† and Yuzuru Ishimura*[4]

**Department of Biochemistry, School of Medicine, Keio University, Shinano-machi, Shinjuku-ku, Tokyo 160-8582; and †The RIKEN Harima Institute/SPring-8, 1-1-1 Kouto, Mikazuki-cho, Sayo, Hyogo 679-5148*

Received August 31, 2000; accepted September 25, 2000

The structure-function relationship in cytochrome P450cam monooxygenase was studied by employing its active site mutant Thr252Ile. X-ray crystallographic analyses of the ferric *d*-camphor–bound form of the mutant revealed that the mutation caused a structural change in the active site giving an enlarged oxygen-binding pocket that did not contain any hydrophilic group such as the OH group of Thr and H_2O. The enzyme showed a low monooxygenase activity of *ca.* 1/10 of the activity of the wild-type enzyme. Kinetic analyses of each catalytic step revealed that the rate of proton-coupled reduction of the oxygenated intermediate of the enzyme, a ternary complex of dioxygen and *d*-camphor with the ferrous enzyme, decreased to about 1/30 of that of the wild-type enzyme, while the rates of other catalytic steps including the reduction of the ferric *d*-camphor–bound form by reduced putidaredoxin did not change significantly. These results indicated that a hydrophilic group(s) such as water and/or hydroxyl group in the active site is prerequisite to a proton supply for the reduction of the oxygenated intermediate, thereby giving support for the operation of a proton transfer network composed of Thr252, Asp251, and two other amino acids and water proposed by previous investigators.

Key words: cytochrome P450cam, oxygen activation, proton transfer, site-directed mutagenesis, X-ray crystallography.

Cytochrome P450 is a generic name given to a family of protoheme proteins that monooxygenate a wide variety of natural and unnatural substrates such as steroids, fatty acids, hydrocarbons, and xenobiotics (*1–3*). Among them, cytochrome P450cam (P450cam) of *Pseudomonas putida* has been the subject of intense mechanistic studies; X-ray crystallographic structures of the enzyme and its site-directed mutants were solved at high resolutions for their various redox and liganded states (*4–9*), and catalytic properties of these enzymes were extensively analyzed (*10*, *11*). The enzyme catalyzes the monooxygenation of *d*-camphor giving 5-*exo*-hydroxycamphor as shown below (*12*).

$$\text{NADH} + d\text{-camphor} + O_2 + H^+ \rightarrow \text{NAD}^+ + \text{5-}exo\text{-hydroxycamphor} + H_2O$$

The reaction is initiated by the binding of *d*-camphor to the ferric resting state of the enzyme, which is then reduced by reduced putidaredoxin (Pdx) to give a ferrous *d*-camphor–bound form of the enzyme. The latter step is hereafter called the 1st electron transfer in this study. Subsequent dioxygen (O_2) binding to the ferrous form yields a *d*-camphor–bound oxygenated ferrous form, the so-called oxygenated intermediate, that decomposes into the reaction products, *i.e.*, the ferric resting states of the enzyme, 5-*exo*-hydroxycamphor and H_2O, upon receiving another electron from reduced Pdx (*13*). The last process is designated as the 2nd electron transfer in the reaction cycle of cytochrome P450.

It has been shown that threonine-252 (Thr252), a highly conserved residue in the heme active center of the cytochrome P450 superfamily, is critical to the catalysis (*14*, *15*). The mutation of Thr252 to a nonhydroxyl amino acid such as Ala or Gly converted the monooxygenase to an oxidase. This enzyme utilizes electrons from NADH to reduce O_2 to H_2O_2, and O-O bond cleavage of O_2 no longer takes place. In other words, the reduction of O_2 was uncoupled from the monooxygenase reaction by the mutation. Hence, it was postulated that the hydroxyl (OH) group provides a

[1] This work was supported in part by Grants-in-Aid for Scientific Research on Priority Areas and Scientific Research (C) from the Ministry of Education, Science, Sports and Culture of Japan, by Special Coordination Funds of the Science and Technology Agency of Japan and by grants from Keio University.

Present addresses: [2] Clinical Research Center, Eisai, Co., Ltd., Koishikawa 4-6-10, Bunkyo-ku, Tokyo 112-8088; [3] Department of Chemistry, College of Science, Rikkyo University, Nishi-ikebukuro 3-34-1, Toshima-ku, Tokyo 171-0021.

[4] To whom correspondence should be addressed. Tel: +81-3-3355-2827, Fax: +81-3-3358-8138, E-mail: yishimur@ med.keio.ac.jp

Abbreviations: P450cam, cytochrome P450cam (CYP101) isolated from *Pseudomonas putida* that catalyzes the conversion of *d*-camphor to 5-*exo*-hydroxycamphor; Pdx, putidaredoxin; PdR, putidaredoxin reductase.

© 2000 by The Japanese Biochemical Society.

Downloaded from http://jb.oxfordjournals.org/ at Peking University on October 1, 2012

proton (H^+) necessary for the O-O bond cleavage in the *d*-camphor monooxygenation reaction (*14*, *16*). However, incorporation of *O*-methyl threonine (CH_3O-Thr), an artificial amino acid, into the 252 position by cell-free protein synthesis yielded an active enzyme with a high coupling ratio, indicating that the O atom but not the H atom (or H^+) in the OH group was necessary for the coupling (*17*). On the other hand, the Ala252- and Gly252-mutants both showed high rates of O_2 reduction that were comparable to that of the wild-type enzyme, although they produce H_2O_2 instead of 5-*exo*-hydroxycamphor and H_2O in the reaction of the wild-type enzyme (*14*, *15*, *18*). Then the elucidation of the crystal structure of ferric Ala252-mutant revealed that an H_2O molecule not present in the wild-type enzyme existed near the O_2 binding site of the mutant (*8*). Questions thus arise as to the roles of Thr hydroxyl and H_2O in the vicinity of the heme active center.

In an attempt to assess this issue, we substituted Ile for Thr at the 252 position, expecting to get a mutant without an OH group or H_2O in the active site. Structural analysis of the mutant in its ferric *d*-camphor–bound state by X-ray crystallography revealed that the mutant was indeed the expected one. Kinetic experiments showed that the mutation caused a remarkable decrease in the O_2 reduction rate and appearance of the activity to produce H_2O_2 from O_2. We also prepared a double mutant, Thr252Ala-Asp251Asn, and examined its catalytic properties. The results were compatible with the view that Thr252 is necessary to keep an H_2O molecule at a suitable position to form a hydrogen bond with O_2 in the oxygenated intermediate, and that the H_2O donates H^+ necessary for a H^+-assisted electron transfer to cleave the O-O bond in the heme-bound O_2.

EXPERIMENTAL PROCEDURES

Preparations of the Enzymes—Genes of the mutant P450cam, Thr252Ile, Thr252Ala, and Asp251Asn-Thr252-Ala, were constructed by using a Takara LA PCR *in vitro* mutagenesis kit with the recommended procedures (Takara, Kyoto). The mutation was confirmed by DNA sequencing and by mass spectrophotometric measurements of lysyl endopeptidase-digests of the purified enzymes. The wild-type and the mutant enzymes were expressed in *Escherichia coli*, strain JM109 and purified by the procedures described previously (*14*). Preparations with an RZ value (A_{391}/A_{280}) greater than 1.6 were employed in this study. Pdx and putidaredoxin reductase (PdR) were purified to homogeneity by SDS-PAGE according to Gunsalus and Wagner (*19*) as described previously (*20*).

Enzyme Assay and Spectrophotometric Measurements—The catalytic activity of the wild-type P450cam and its mutants was measured in a reconstituted system composed of Pdx, PdR, and the enzyme at 20°C as described (*14*) with minor modifications. The assay mixture contained 14 μM Pdx, 0.12 μM PdR, 360 μM NADH, and 0.036 μM wild-type enzyme or an appropriate concentration of a mutant in 50 mM K phosphate buffer, pH 7.4, containing 50 mM KCl and 1 mM *d*-camphor (hereafter called standard buffer). The amount of 5-*exo*-hydroxycamphor was determined by gas chromatography and that of H_2O_2 was calculated from the amount of oxygen evolved by the addition of catalase to the reaction medium after the reaction had been terminated by adding an excess amount of metyrapone (*14*). Spectrophotometric measurements were carried out with a Perkin Elmer UV/VIS spectrometer, model lambda 18 (Uberlinger, Germany). The equilibrium binding of *d*-camphor to the ferric form of various types of P450cam was measured on the same spectrophotometer by the method of Peterson (*21*) with slight modifications. More details are described under appropriate figure legends.

Kinetic Experiments—Rapid reactions were carried out with a Unisoku stopped-flow/rapid scan spectrophotometer, model RSP-601 (Osaka) as described previously (*20*). Both association and dissociation rate constants (k_{on} and k_{off}, respectively) of *d*-camphor for the *d*-camphor complex of ferric wild-type P450cam and its mutants were measured according to Griffin and Peterson (*22*) with minor modifications. To measure the k_{off} one reservoir of the stopped-flow apparatus contained 5 μM ferric *d*-camphor–bound form of the enzyme in 50 mM K phosphate, pH 7.4, containing 50 mM KCl and 0.1 mM *d*-camphor, while the other contained an excess amount of metyrapone (up to 8 mM) in 50 mM K phosphate, pH 7.4, containing 50 mM KCl. Neither the enzyme nor *d*-camphor was contained in the latter. After mixing, formation of ferric metyrapone complex of the enzyme was followed by measuring the increase in absorbance at 420 nm; the *d*-camphor–free form of the enzyme produced by the dissociation reaction was trapped as a stable complex of metyrapone with enzyme (*22*). The k_{on} was determined as described elsewhere (*22*).

The rate of reduction of ferric P450cam and its mutants by reduced Pdx was measured as reported previously (*20*) based on the method of Hintz and Peterson (*23*). Usually, one reservoir of the stopped-flow apparatus contained 2 μM ferric form of the enzyme in the standard buffer and the other reservoir contained 5–60 μM reduced Pdx in the same buffer containing 1 mM carbon monoxide (CO), which trapped the ferrous form generated by the reaction. The formation of a CO ferrous form was followed spectrophotometrically. The observed rates (k_{obs}) *versus* concentrations of Pdx added to the reaction mixture were analyzed by the method of Davies and Sligar (*24*) to obtain the rate of intracomplex electron transfer from reduced Pdx to ferric form of the enzyme. The rate of degradation of the oxygenated intermediate to the ferric resting form and the reaction products was measured at 4.5 ± 0.5°C as described elsewhere (*20*) by mixing 4 μM oxy-ferrous wild-type P450cam or its mutants in one reservoir with 10–100 μM reduced Pdx in another reservoir that contained 5 mM metyrapone as a trapping agent for the ferric *d*-camphor–free form of P450cam (*25*). The results were analyzed according to Davies and Sligar (*24*).

On the same rapid mixing apparatus, the rate constants for O_2 binding (k_{on}) and O_2 dissociation (k_{off}) from oxy-ferrous form of the wild-type and mutant enzymes were determined at 4.5 ± 0.5°C by measuring the rate of O_2 binding to 2.5 μM enzyme with 55, 110, and 230 μM O_2 in the standard buffer. The observed rates increased linearly as the concentration of O_2 was raised. From linear regression analyses of the results, we obtained k_{on} and k_{off} from the slope and the intercept on the coordinate of the plot, respectively.

Crystallization and X-Ray Crystallography—The wild-type and Ile252-mutant enzymes were crystallized as described by Poulos and his coworkers (*26*) with minor modifications. The crystallization was initiated by layering 0.02

Downloaded from http://jb.oxfordjournals.org/ at Peking University on October 1, 2012

ml of 750–850 μM mutant P450cam containing 0.05 M DTT over an equal volume of $(NH_4)_2SO_4$ solution at 0.58–0.62 saturation in microtubes (4 × 30 mm), while that of the wild-type was done with 850–950 μM protein and $(NH_4)_2SO_4$ solution at 0.65–0.70 saturation. The tubes were sealed with Parafilm® (American National Can) and stored at 20°C. Brown crystals began to appear after 1 or 2 days. The crystals were grown for 1 or 2 more days to about 0.1–0.3 mm in length and transferred to a 50% saturated $(NH_4)_2SO_4$ solution containing 1 mM *d*-camphor. Analysis of diffraction images showed that the crystals of the recombinant enzymes were isomorphous with those of the native P450cam. The data were obtained at the synchrotron radiation source of the BL44B2 (RIKEN Beam Line 2) station in the SPring-8, Harima (*27*). All data sets were collected on R-AXIS IV imaging plates as a detector. Diffraction data were integrated and scaled with the Mosfilm (*28*) and Scala (*29*). Statistics of the data collection are given in Table I. The atomic model was built using the program TURBO-FRODO (*30*), and improved with Sigma A-weighted $|2F_o–F_c|$ and $|F_o–F_c|$ maps iteratively with X-PLOR (Brunger). The structure of the native P450cam in the $P2_12_12_1$ space group (PDB ID: 2CPP), without the coordinates of *d*-camphor and H_2O molecules, was used as an initial model for refinement of the structures of the wild-type and The252Ile mutant. After the first round of rigid-body, simulated annealing and B-factor refinements, a $|2F_o–F_c|$ map was calculated. High electron density was found for the *d*-camphor molecule. After manual rebuilding of the *d*-camphor and H_2O molecules, other rounds of refinement were done, in which positional, individual B-factors and bulk solvent correction of the protein model were included. H_2O molecules were placed at positions where spherical densities were above 1.5σ in the $|2F_o–F_c|$ map and above 3.0σ in the $|F_o–F_c|$ map, and where the stereochemically reasonable hydrogen bonds were allowed. Structural evaluations of the final models of the wild-type and Ile252-mutant enzymes using PROCHECK (*31*) indicated that 90–91% of the residues were in the most favorable regions of the Ramachandram plot, and no residues were in disallowed regions. The coordinates of the the Ile252-mutant P450cam have been submitted to the PDB (we will report the ID codes as soon as they are received).

RESULTS

X-Ray Structure of Ile252-Mutant—The X-ray crystallographic structure of ferric *d*-camphor–bound form of Thr-252Ile-mutant P450cam was determined at 2.0 Å resolution. The structure of the wild-type P450cam purified and crystallized by our procedures was also determined at the same resolution in order to confirm that the results obtained for the Ile252-mutant were caused by amino acid substitution of the wild-type enzyme. The structure of the wild-type enzyme was found to be almost indistinguishable from that reported by Poulos *et al.* (*5*), and that of the Ile252-mutant was as a whole strikingly similar to the structure of the wild-type. When active site structures of the wild-type and mutant proteins were compared, however, a remarkable difference was noted in their oxygen-binding pockets, a space which accommodates molecular O_2 bound to the heme iron in the ferrous *d*-camphor–bound form of the wild-type enzyme (*5*). As seen in Fig. 1A, the pocket (marked by an asterisk) in the wild-type enzyme was surrounded by a wall composed of amino acid residues Gly248 and Thr252 of the I-helix, the bound substrate molecule (*d*-camphor), and the heme plane. In the amino acid wall, Gly248 and Thr252 were connected with each other by a hydrogen bond between the carbonyl oxygen of the glycine and the OH of the threonine side chain. Such a hydrogen bond could no longer exist in the Ile252-mutant because it lacks a hydrogen donor in the side chain. Thus the mutation caused a break of the wall resulting in an enlargement of the O_2-binding pocket as shown in Fig. 1B.

TABLE I. **Crystal parameters, data collection and structure refinement.**

Data set	Wild-type	T252I
Resolution range (Å)	15.0–2.0	30.0–2.03
Unit cell dimensions (Å)	a = 109.12, b = 104.33, c = 36.18	a = 106.67, b = 103.44, c = 34.99
Reflections		
Measured/unique	106,959/27,250	108,401/26,966
Completeness (%)		
Overall/outer shell (2.11–2.00)	95.1/79.8	99.9/99.8
R_{merge} (%)[a]		
Overall/outer shell (2.11–2.00)	3.2/6.1	6.0/21.1
Redundancy	3.9	4.0
Refinement statistics		
Resolution range (Å)	15.0–2.0	30.0–2.03
σ cut-off	0.0	0.0
Reflections used	27,147	26,764
R-factor (%)[b]	17.7	18.6
Free *R*-factor (%)	21.6	22.8
Solvent	187	100
Rms deviations from ideals		
Bond lengths (Å)	0.007	0.006
Bond angles (degrees)	1.141	1.155
Ramachandran plot		
Residues in most favorable regions (%)	91.1	89.9
Residues in additional allowed regions (%)	8.9	10.1
Residues in disallowed regions (%)	0.0	0.0

[a] $R_{merge} = \Sigma|I_i–\langle I\rangle| / \Sigma|I_i|$, where I_i is the intensity of the ith observation and $\langle I\rangle$ the mean intensity for that reflection; the summations are over all reflections. R_{free} was calculated with 5% of the data. [b] *R*-factor = $\Sigma_h||F_o(h)|–|F_c(h)|| / \Sigma_h|F_o(h)|$, where F_o and F_c are, respectively, the observed and calculated structure factor amplitudes for the reflection h.

Downloaded from http://jb.oxfordjournals.org/ at Peking University on October 1, 2012

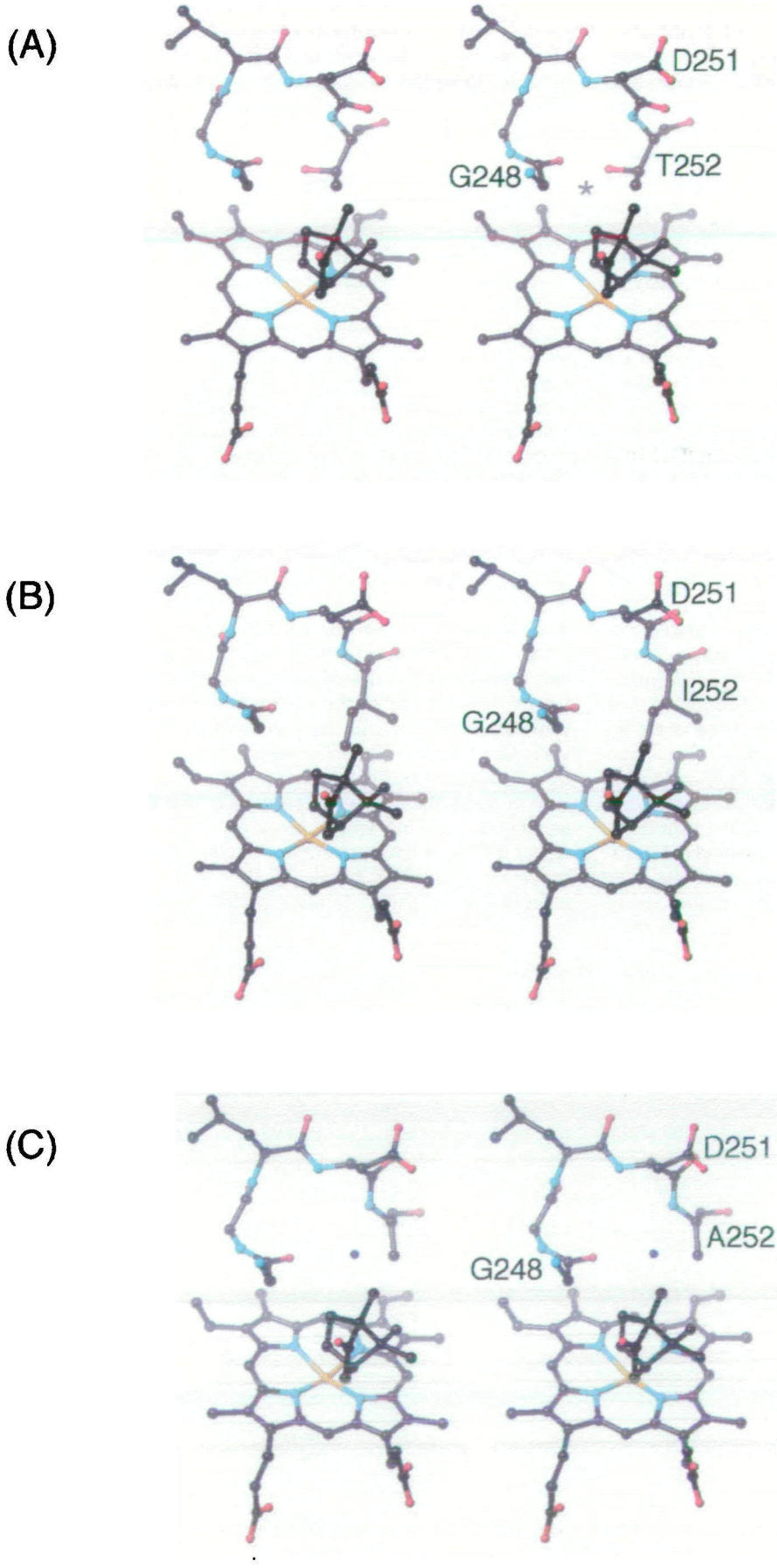

Fig. 1. **Active site structures of ferric *d*-camphor–bound forms of the wild-type P450cam (A) and its mutants, Thr252-Ile (B), and Thr252Ala (C).** The heme, the bound-substrate (*d*-camphor) and a part of the distal I-helix between the residues 248 to 252 (Gly248-Gly249-Leu250-Asp251-Thr/Ile/Ala252) are presented in the figure by a dark gray stick and ball model with oxygen and nitrogen atoms colored red and light blue, respectively. The asterisk in panel A indicates the oxygen-binding pocket, a space that accommodates molecular O_2 bound to the heme iron in the ferrous *d*-camphor–bound form of the wild-type enzyme (*5*). A blue sphere in panel C represents a water molecule in the oxygen pocket found only in the Ala252-mutant. The coordinates for the Ala252-mutant (*8*) were taken from the PDB (the assigned number 2CP4).

Downloaded from http://jb.oxfordjournals.org/ at Peking University on October 1, 2012

A similar and even greater enlargement of the pocket was observed in another 252-mutant, Thr252Ala (*8*), the coordinates of which were taken from the PDB and are shown in Fig. 1C. Associated with these changes, the side chain β-carbon of Ile or Ala at the 252-position shifted away from the pocket as compared to that of Thr252 at the same position, and the carbonyl group of Asp251, the preceding residue in the I-helix, turned away from the O_2 pocket and toward the I-helix in both cases. Interestingly, a similar move of the β-carbon and a turnaround of the carbonyl group of Asp251 were observed upon oxygenation of the ferrous *d*-camphor–bound form of the wild-type enzyme (*7*). In the Ile252-mutant, furthermore, the side chain of Ile was found to extend from the original Cβ position toward the heme-iron, and the terminal methyl group (Cδ) of Ile252 was in a van der Waals contact with the bound-substrate, *d*-camphor (data not shown).

Figure 2 compares the distribution of H_2O molecules (blue sphere) in and around the active site of the wild-type (A), Ile252-mutant (B), and Ala252-mutant enzymes (C). Again, the coordinates for the structure of the Ala252-mutant (*8*) were taken from the PDB. In all three cases, a H_2O molecule (arrowhead) was found outside the oxygen pocket and behind the 251 and 252 residues, while an additional H_2O was present inside the pocket only in the Ala252-mutant (thin arrow). An asterisk marks the hydroxyl oxygen of Thr252 in the wild-type in A. Thus the wild-type and Ala-mutant enzymes possess a OH group and a H_2O molecule, respectively, within their active site, while the Ile252-mutant contains no such a hydrophile which can serve as a hydrogen donor or acceptor upon formation of a hydrogen bond. The H_2O molecules commonly found outside the active site in all the three proteins were found to link with a buried Glu366-residue *via* two internal H_2O molecules by hydrogen bonding, in agreement with the previous findings on the wild-type and Ala252 enzymes (*5*, *8*).

Spectral Properties—The UV and visible absorption spectra of ferric, ferrous, oxy-ferrous and ferrous CO forms of the Ile252-mutant in the presence of *d*-camphor are shown in Fig. 3. Typical of the spectra of the P450 superfamily, they were indistinguishable from those of the wild-type enzyme; all absorption maxima and isosbestic points were at the same wavelengths as those of the wild-type enzyme. The results thus support the view described above that the structure of the Ile252-mutant was as a whole very similar to that of the wild-type P450cam. As will be described later, the oxy-ferrous *d*-camphor–bound form, *i.e.*, the oxygenated intermediate, of the Ile252-mutant was less stable than that of the wild-type enzyme, as judged from the stability of the 418 nm peak.

Catalytic Properties—In contrast to the spectral properties, the catalytic activity showed substantial changes as a result of mutation. As shown in Table II, O_2 consumption rate decreased to 277 min^{-1} in the Ile252-mutant from the 1,350 min^{-1} of the wild-type enzyme. The value was the smallest among those of the 252-mutants listed in the table except for that of the double mutant Thr252Ala-Asp251-Asn, which was only 5 min^{-1}. The coupling ratio of the O_2 consumption to the monooxygenation (*14*) also dropped to 44% from 100% of the wild-type enzyme. Hence, the monooxygenase activity of this mutant to form 5-*exo*-hydroxycamphor was less than 1/10 of the activity of the wild-type

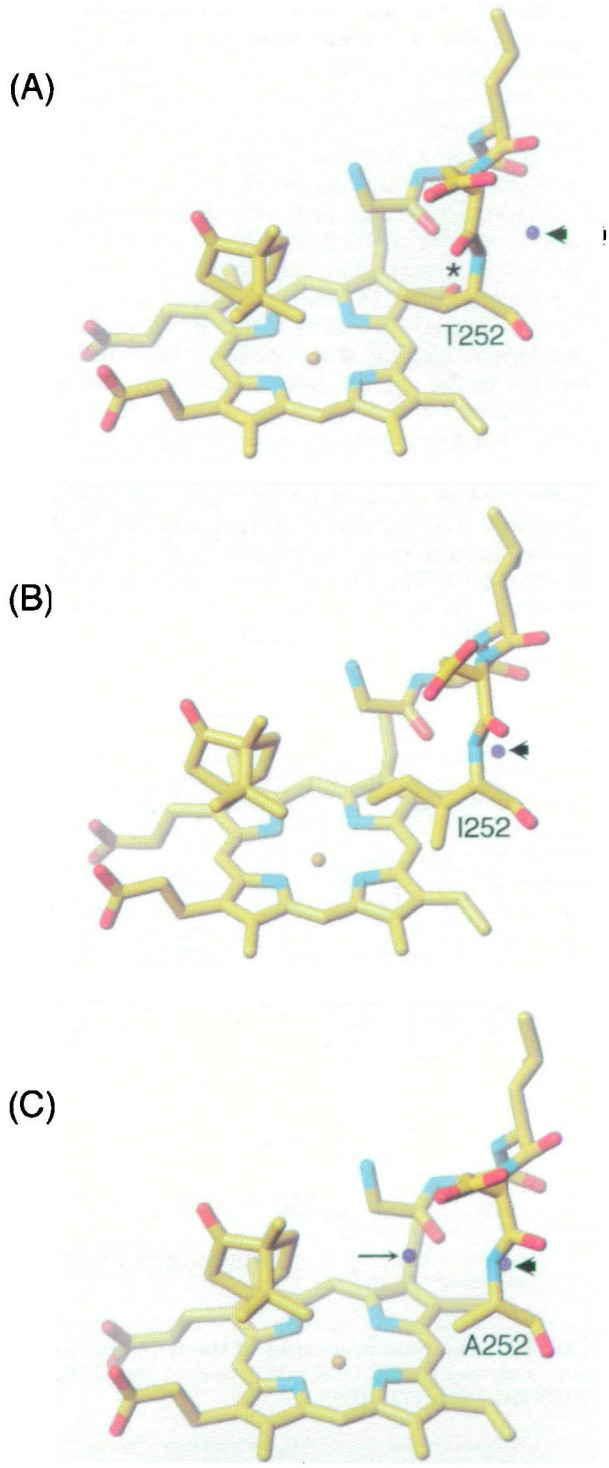

Fig. 2. **Water molecules (dark blue spheres) in and near the active center of ferric *d*-camphor–bound forms of the wild-type P450cam (A) and its mutant, Thr252Ile (B) and Thr252-Ala (C).** The structures are those in Fig. 1, but viewed from the right side. The arrowhead in each panel shows a water molecule common to the three proteins outside of the oxygen pocket. The water links with a buried Glu366 *via* two internal water molecules by hydrogen bonding (data not shown). The asterisk in panel A indicates the hydroxyl of Thr252. In the Ala252-mutant, the thin arrow indicates an additional water molecule in the active site. The coordinates for the Ala252-mutant (*8*) were taken from the PDB (the assigned number 2CP4). Other details are in Fig. 1.

Downloaded from http://jb.oxfordjournals.org/ at Peking University on October 1, 2012

enzyme, *ca.* 120 min^{-1}. H_2O_2 producing activity was calculated to be *ca.* 110 min^{-1}. It should be noted here that all the enzymes in the table with a relatively high O_2 consumption rate (830–1,350 min^{-1}), *i.e.*, wild-type, Thr252Ala, Thr252Gly, and Thr252Ser, are considered to have either a OH group or a H_2O molecule in their active site, while Thr252Ile has neither, as we proved in the X-ray crystallographic structure. This point as well as the low oxygen consuming activity of the double mutant, Thr252Ala-Asp251-Asn, will be discussed in more detail later.

Association and Dissociation Reactions of d-Camphor—We next studied the effects of mutation on the equilibrium and kinetic binding of *d*-camphor with the ferric Ile252-mutant. In Fig. 4A, the observed rates, k_{obs}, for the binding of *d*-camphor with ferric forms of both the wild-type and Ile252-mutant enzymes were plotted against the concentration of *d*-camphor, where the slopes of the plots correspond to the rate of *d*-camphor binding, k_{on}, with the enzymes. The value of 5×10^6 M^{-1} s^{-1} obtained for the Ile252-mutant was comparable to 6×10^6 M^{-1} s^{-1} for the wild-type enzyme at 4.5 ± 0.5°C. The latter value was also in good agreement with that reported by Griffin and Peterson for the wild-type enzyme (4.1×10^6 M^{-1} s^{-1} at 4°C) (*22*). Thus the rate of *d*-camphor binding to ferric P450cam was scarcely affected by the mutation.

On the other hand, the rate of dissociation, k_{off}, of *d*-camphor was significantly affected by the mutation as shown in Fig. 4B, where the k_{obs} for the metyrapone binding at its saturated concentration (*ca.* 4 mM) corresponded to k_{off} of *d*-camphor from the ferric *d*-camphor complex of P450cam. The k_{off} value 2.5 s^{-1} thus obtained for the Ile252-mutant was smaller than that found for the wild-type enzyme, 10 s^{-1}, by a factor of 4 at 4.5 ± 0.5°C. Then, based on the k_{on} and the k_{off} values, the equilibrium dissociation constant, K_d, of *d*-camphor was calculated for the wild-type and Ile252-mutant to be 1.7×10^{-6} and 5×10^{-7} M, respectively. These also differ by a factor of 4, reflecting the difference in the k_{off} values. These results, obtained in 50 mM K phosphate buffer, pH 7.4, containing 50 mM KCl at 4.5°C, are summarized in Table III.

K_d value of *d*-camphor was also determined at 10°C by measuring the equilibrium binding of *d*-camphor with the enzymes in the absence of K^+ ion as shown in Fig. 4C. The values obtained were 7.9 and 2.4×10^{-6} M for the wild-type and Ile252-mutant, respectively (see also Table III). Here again the Ile252-mutant showed a higher affinity toward *d*-camphor by a factor of 3, despite the differences in temperature and buffer components from the kinetic experiments

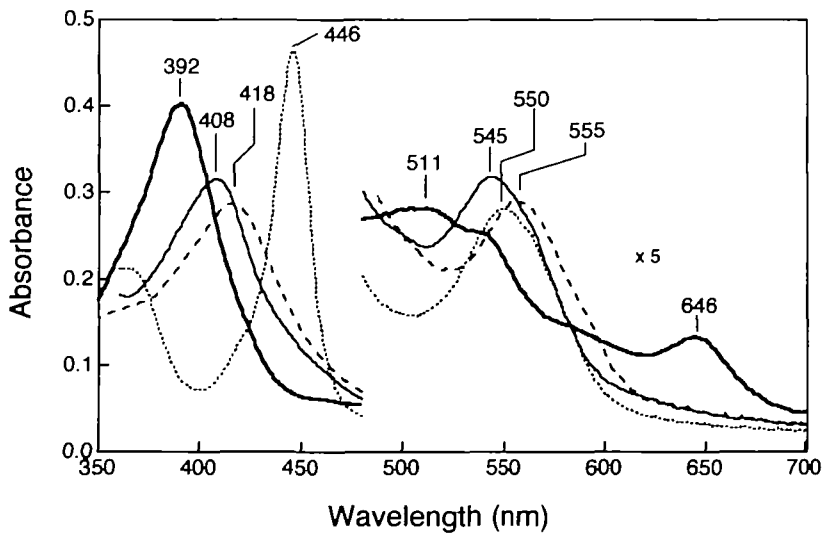

Fig. 3. **Absorption spectra of the Ile252-mutant cytochrome P450cam.** The spectra of 3.9 μM P450cam were obtained in 50 mM potassium phosphate, pH 7.4, containing 50 mM KCl and 1 mM *d*-camphor. A ferric form of the Ile252-mutant (thick solid line) was reduced with solid sodium dithionite to the ferrous form (thin solid line). Ferrous-CO (dotted line) was prepared by a gentle bubbling of CO gas into a dithionite-reduced ferrous form, while ferrous-O_2 (dashed line) form was obtained by mixing the ferrous form with the above buffer saturated with air. The spectra were all recorded at 20°C except for the oxy-ferrous form, which was taken at 4.5 ± 0.5°C. Numbers in the figure represent wavelength in nm for the absorption peaks of the spectra.

TABLE II. **Catalytic properties of the wild-type and mutant P450cam enzymes.** Oxygen consumption rates for various P450cams were measured at 20°C in 50 mM potassium phosphate, pH 7.4, containing 50 mM KCl and 1 mM *d*-camphor as described in the "EXPERIMENTAL PROCEDURES."

P450cam species	O_2 consumption rate (min^{-1})	Products formed per O_2 consumed (%)		Source (Ref.)
		5-OH-CAM†	H_2O_2	
Wild-type	1350	100	3	This work
T252I	277	44	40	This work
T252A D251N	5	52	64	This work
Wild-type	1350	97	3	*18*
T252G	1090	3	88	*18*
T252A	1150	5	89	*18*
T252S	830	85	15	*18*
D251G	21	99	2	*18*
D251A	3	89	12	*18*
D251N	6‡	90	—	*16*

†5-OH-CAM, 5-*exo*-hydroxycamphor. ‡The oxygen consumption rate for the wild-type P450cam was reported to be 822 min^{-1} (*16*).

Downloaded from http://jb.oxfordjournals.org/ at Peking University on October 1, 2012

described above. The fact that the mutation decreased the *d*-camphor *off*-rate without affecting the *on*-rate may indicate that a bulky hydrophobic side chain of Ile252 did not interfere with the *d*-camphor binding, but rather stabilized the bound *d*-camphor molecule through the van der Waals contacts.

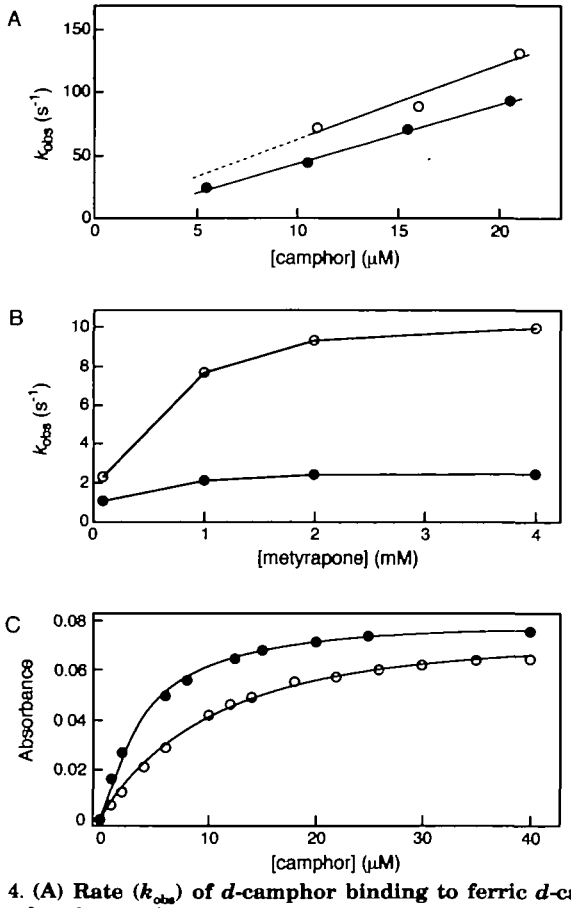

Fig. 4. **(A) Rate (k_{obs}) of *d*-camphor binding to ferric *d*-camphor–free forms of the wild-type (open circle) and Ile252-mutant (closed circle) enzymes *versus* concentration of *d*-camphor.** The association rate constant (k_{on}) was determined from the slope obtained by a linear regression analysis of the rates (k_{obs}). **(B) Rate (k_{obs}) of metyrapone binding to ferric *d*-camphor–free form of the wild-type (open circle) and Ile252-mutant (closed circle) enzymes that initially associated with *d*-camphor *versus* concentration of metyrapone.** As the concentration of metyrapone increased, the rate approached the *d*-camphor–off rate from *d*-camphor–bound ferric form. **(C) Equilibrium binding of *d*-camphor to ferric *d*-camphor–free form of the wild-type (open circle) and the Ile252-mutant (closed circle) enzymes.** Other details are described under "EXPERIMENTAL PROCEDURES."

The First Electron Transfer and Dioxygen (O_2) Binding—Since the small changes in *d*-camphor binding parameters upon the mutation did not explain the large changes in the catalytic activity, we examined the effects of the mutation at the 252-position on further steps of the catalytic reaction. First, the reduction rate of ferric Ile252-mutant by reduced Pdx was studied by monitoring the formation of the CO ferrous form at 446 nm in the presence of excess amounts of CO and *d*-camphor. The time course of the reduction, *i.e.*, the formation of the CO ferrous form, followed first-order kinetics (*20*). The apparent rate (k_{obs}) obtained from the time course increased linearly as the concentration of Pdx was raised (data not shown) and reached a plateau at the Pdx concentration of 10–20 μM (Fig. 5A). The k_{obs} values calculated at infinite concentration of Pdx for the wild-type and Ile252-mutant enzymes were almost identical, 33 and 32 s^{-1}, respectively. These results together indicate that the mutation of Thr252 to Ile has no effect on the rate of reduction of the ferric enzyme, and that the rate-determining step in the reduction was that of the intracomplex electron transfer from reduced Pdx to the ferric enzyme in the complex. The latter interpretation supports the conclusion of Hintz and Peterson (*32*).

O_2 binding to the ferrous form follows subsequent to the reduction of the ferric form by reduced Pdx in the catalytic reaction. The rate constants for O_2 binding (k_{on}) and its dissociation (k_{off}) from oxy-ferrous Ile252-mutant were determined by measuring the apparent O_2 binding rate at various concentrations of O_2. The results showed that k_{on} and k_{off} of the mutant were 8.2×10^5 M^{-1} s^{-1} and 40 s^{-1}, respectively, while those of the wild-type enzyme to be 7.4×10^5 M^{-1} s^{-1} and 6.7 s^{-1}, respectively. Thus, the mutation did not change the O_2 association rate significantly, suggesting that the side chain of Ile was in a position not to hinder the O_2 binding to the heme in the ferrous *d*-camphor–bound form of the enzyme, while it increased the dissociation rate by 6-fold (see "DISCUSSION"). The results are summarized in Table III.

The 2nd Electron Transfer and Autooxidation of the Oxygenated Intermediate—Finally, we determined the rate of degradation of the oxygenated intermediate, a ternary complex of O_2, *d*-camphor and the ferrous form of the Ile252-mutant, upon reaction with reduced Pdx. The degradation regenerated the ferric form of the enzyme yielding the three reaction products, 5-*exo*-hydroxycamphor, H_2O and/or H_2O_2. The reaction was followed by measuring the formation of ferric metyrapone complex of the enzyme at 420 nm

TABLE III. **Kinetic properties of the wild-type and mutant P450cams.** Kinetic data were obtained in 50 mM potassium phosphate, pH 7.4, containing 50 mM KCl and 1 mM *d*-camphor, at 4.5 ± 0.5°C, unless indicated otherwise. Other details were described in the "EXPERIMENTAL PROCEDURES."

P450cam species	1st electron transfer	2nd electron transfer	Camphor binding			Oxygen binding			Autooxidation
	k_{ET1} (s^{-1})	k_{ET2} (s^{-1})	k_{on} ($\mu M^{-1} s^{-1}$)	k_{off} (s^{-1})	K_d (μM)	k_{on} ($\mu M^{-1} s^{-1}$)	k_{off} (s^{-1})	K_d[b] (μM)	k (s^{-1})
Wild-type	33[a]	189	6	10	1.7[b] 7.9[c]	0.74 1.1[d]	6.7 25[d]	9.1 22[d]	5.3×10^{-4}
T252I	32[a]	6.7	5	2.5	0.5[b] 2.4[c]	0.82	40	49	2.8×10^{-3}
T252A			8	15	1.9[b]	0.51[d]	12[d]	24[d]	4.0×10^{-3}

[a]Data at 20°C. [b]Values were calculated from k_{on} and k_{off} according to an equation $K_d = k_{off}/k_{on}$. [c]Data from the equilibrium binding of *d*-camphor to ferric camphor-free P450cam in 50 mM Tris-HCl, pH 7.4 at 10°C. [d]Data at 15°C.

Downloaded from http://jb.oxfordjournals.org/ at Peking University on October 1, 2012

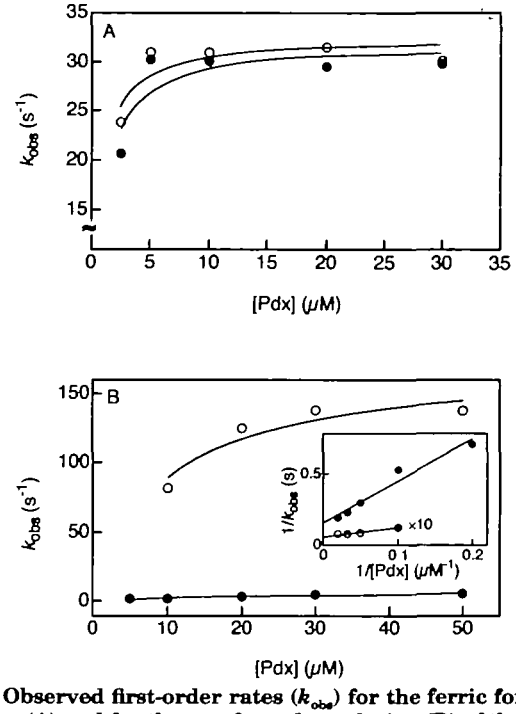

Fig. 5. **Observed first-order rates (k_{obs}) for the ferric form reduction (A) and for the oxy-form degradation (B) of the wild-type (open circle) and Ile252-mutant (closed circle) enzymes by reduced putidaredoxin *versus* concentration of reduced putidaredoxin.** The rates were obtained from a single exponential fitting to the time courses. The rate was an average of 3–7 measurements. Inset in B, the Lineweaver-Burk plots of k_{obs} at various concentrations of Pdx. The maximum rates were obtained from intercepts on the coordinate. Other details are described under "EXPERIMENTAL PROCEDURES."

in the presence of an excess amount of metyrapone (*25*). The time course of the reaction followed a single exponential profile as described previously (*33*), and the observed rates (k_{obs}) were plotted against the concentration of reduced Pdx as shown in Fig. 5B. As seen, the rate for the Ile252-mutant was markedly smaller than that for the wild-type in the range of Pdx concentrations tested. The maximum conversion rate obtained from the Lineweaver-Burk plots of the results (see the inset of Fig. 5B) was 6.7 s^{-1} for the Ile252-mutant, while that of the wild-type P450cam was 189 s^{-1}. The mutation of Thr252 to Ile was thus found to reduce the 2nd electron transfer rate to about 1/30. As described above, the mutation did not change the rate of the 1st electron transfer significantly. These asymmetric effects of the mutation on the 1st and 2nd electron transfer were the most prominent findings in the reaction catalyzed by Ile252-mutant of P450cam. The rate of autooxidation of the oxygenated intermediate increased by 6-fold as also shown in Table III. The cause of this phenomenon is discussed below in relation to the structure.

DISCUSSION

The active site of Ile252-mutant of P450cam has a larger O_2-binding pocket than that of the wild-type, but does not contain a hydrophilic group such as the OH group of Thr and H_2O found in the wild-type and Ala252-mutant enzymes, respectively. Thus the Ile252-mutant can be used to examine the roles of these hydrophilic molecules in the active site of P450cam monooxygenase. In its catalytic properties, the Ile252-enzyme showed a small O_2 consumption rate that was less than 1/5 of the wild-type enzyme. All other 252-mutants in Table II except for the double mutant Ala252-Asn251 exhibited a much higher O_2 consumption rate than the present mutant. It appears therefore that the presence of a hydrophilic group, *i.e.*, an OH group or H_2O, is prerequisite for the high O_2 consumption. In the same context, a decrease in the oxygen consumption rate to 1/3 of the wild-type upon mutation of Thr252 to Val (*14*) can be interpreted as resulting from a possible lack of the hydrophilic group in the active site.

The decrease in oxygen consumption rate measured in the reconstituted system, however, does not specify which step in the whole catalytic cycle was affected by the mutation. In the Ile252-mutant, the rate of degradation of the oxygenated intermediate, *i.e.*, the 2nd electron transfer rate, was found to change most prominently: it dropped to 6.7 from 189 s^{-1} of the wild-type enzyme. It was also comparable to the rate of overall oxygen consumption of the Ile-mutant (277 min^{-1}). These results suggest that the rate-limiting step in the overall catalysis is the degradation of the oxygenated intermediate, whereas in the wild-type enzyme it is the 1st electron transfer, as will be described below. As shown in Fig. 5, A and B, the rate of the latter reduction (*ca.* 30 s^{-1}) was much slower than the former (120–150 s^{-1}) at the reduced Pdx concentration of 20 to 50 μM. Moreover, the rate of the 1st electron transfer was comparable to the oxygen consumption rate for the wild-type enzyme (23 s^{-1}), suggesting that it is the rate-limiting step in the overall catalysis (*14*). The Ile252-muant was the first enzyme that showed a slow 2nd electron transfer rate among the mutant enzymes that had an amino acid substitution only at position 252 of P450cam.

In contrast to the remarkable decrease in the rate of the 2nd electron transfer, the rate of the 1st electron transfer was not affected by the mutation: 32 and 33 s^{-1} for the Ile252-mutant and wild-type enzymes, respectively (see Table III). The question thus arises of by what mechanism the mutation exerted such an asymmetric effect on the 1st and the 2nd electron transfer reactions. Both 1st and 2nd electrons were provided by the same electron donor, reduced Pdx.

It should be recalled here that the first electron transfer reduces the heme-iron from the ferric (Fe^{III}) to the ferrous state (Fe^{II}), while the 2nd electron transfer decomposes the oxygenated intermediate, a ternary complex of O_2, *d*-camphor and the ferrous enzyme. The latter process is thought to involve proton transfer reactions, and is known to be the only step that displays a kinetic solvent isotope effect among the reactions in the catalytic cycle of P450cam (*9*, *34*). On the other hand, no such an isotope effect has been observed for the 1st electron transfer.

Such an asymmetric effect of a mutation on the 1st and the 2nd electron transfer reactions of P450cam is not unique to the Ile252-mutant, but has also been found for the mutants at Asp251. As shown in Fig. 6, the Asp251 residue plays a crucial role in the specific proton delivery network proposed for the active site of P450cam (*9*, *17*, *35*). When the Asp251 was mutated to non-ionizable amino acids such as Ala or Asn, the 2nd electron transfer rate became sluggish, while the 1st electron transfer rate was

Downloaded from http://jb.oxfordjournals.org/ at Peking University on October 1, 2012

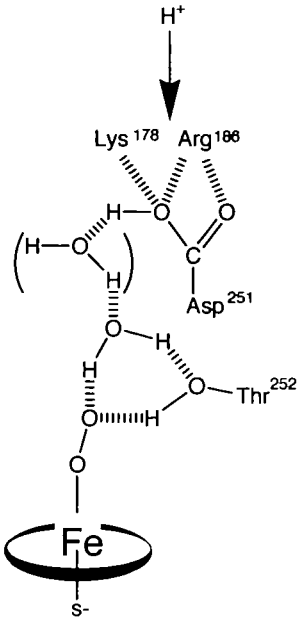

Fig. 6. **A proposed proton delivery system in P450cam.** We have proposed a proton delivery system composed of Thr252-H_2O-Asp251-Lys178/Arg186 linked *via* hydrogen bonding (▮▮▮) (*36*). H_2O at the terminus of the system serves as an acid catalysis/proton donor for the cleavage of heme-bound O_2 (*17*). In our model, Asp delivers a proton to the terminal H_2O possibly *via* one more H_2O.

totally unchanged (*35*, *36*). The results can therefore be interpreted to mean that the mutation of Asp251 to a nonfunctional amino acid disrupts the proton delivery network and blocks the 2nd electron transfer, which is coupled to the proton transfer. Such coupling of proton transfer to electron transfer is known as proton-assisted electron transfer (*37*). By the same token, the present finding that the mutation of Thr252 to Ile affected only the 2nd electron transfer can be interpreted to mean that the mutation decreased the rate of proton delivery, thereby depressing the 2nd electron transfer reaction, which is coupled to the proton transfer. The 1st electron transfer, *i.e.*, a reduction of ferric (Fe^{III}) to ferrous (Fe^{II}) heme iron, cannot be affected by the mutation, since it does not require proton(s) associated with the reaction.

The hydrogen bond network linking the OH group of Thr252, heme-bound O_2 and H_2O in Fig. 6 has recently been confirmed by an X-ray crystallographic study on the oxygenated intermediate of the wild-type enzyme by Schlichting *et al.* (*7*). Accordingly the OH group of Thr252 is thought to stabilize both heme-bound O_2 and the terminal H_2O perhaps in a manner to facilitate the monooxygenase reaction, *i.e.*, the O-O bond scission. As mentioned, however, the OH group of Thr252 does not serve as the proton donor to the heme-bound O_2. The functional proton which facilitates the O-O bond cleavage is therefore considered to be given by the terminal H_2O. Upon mutation of Thr252 to Ile, on the other hand, the specific proton delivery machinery in Fig. 6 must be impaired at least in part, resulting in a slow proton transfer, which further decreases the electron transfer rate. At the same time, the destabilization of both terminal H_2O and heme-bound O_2 due to the losses of hydrogen bonds may result in the production of H_2O_2 through a disordered proton delivery.

In contrast to Ile252-mutant, both Ala252- and Gly252-mutants displayed high O_2 consumption rates comparable to the wild type, although the product from O_2 was mostly H_2O_2 (Table II). The results indicated that proton transfer rate remained high, and hence electron transfer rate was high in these mutants. When the Ala252-mutant was further converted to a double mutant, Ala252-Asn251, however, the rapid O_2 consumption rate dropped by two orders of magnitude to the same level as in the single mutants at the 251-position (Table II). The results thus indicate that the Asp251 residue is also responsible for the proton transfer in the Ala252-mutant, and that it is H_2O that provides a proton to the heme-bound O_2 to cleave the O-O bond.

The present study also showed that the mutation of Thr252 to Ile accelerated the O_2 off-reaction by 4-fold and the rate of autooxidation by 5-fold (Table III). As mentioned earlier, the heme-bound O_2 forms a hydrogen bond with the OH of Thr in the oxygenated intermediate of the wild-type P450cam (*7*). In the mutant protein, however, no such hydrogen bond can be formed, because of the lack of the OH group, and this results in the increases in the off and autooxidation rates. It is well established that the heme-bound O_2 in myoglobin interacts with nearby distal His through a hydrogen bond, resulting in a remarkable reduction in the O_2 off-rate (*38*). The mechanisms for the autooxidation of the oxygenated form of heme proteins have been the subject of extensive studies employing the native and mutant myoglobins (*39*). According to the proposed mechanism, H_2O in the active site of the Ala252-mutant facilitates protonation of the bound O_2, generating $Fe^{II}(O_2H)^+$, which dissociates into Fe^{III} and HO_2.

Finally, it appears that an H_2O molecule that serves as the proton donor for the heme-bound O_2 in the proton delivery network is present in the active site of P450cam. The role of the OH group of Thr252 is considered to be to stabilize both heme-bound O_2 and the active site H_2O through hydrogen bonding. The present discussions are, however, based mainly on the structural findings obtained for the ferric forms of the mutant enzyme. The elucidation of structures of the oxygenated forms of several mutant enzymes such as Thr252Ala and Thr252Ile is necessary to obtain an unambiguous answer.

We are grateful to Ms. Yoko Minowa for her excellent technical assistance.

REFERENCES

1. Waterman, M.R., John, M.E., and Simpson, E.R. (1986) Regulation of synthesis and activity of cytochrome P450 enzymes in physiological pathways in *Cytochrome P450: Structure, Mechanism and Biochemistry* (Oritiz de Montellano, P.R., ed.) pp. 345–386, Plenum Press, New York and London
2. Capdevila, J.H., Zeldin, D., Makita, K., Karara, A., and Falck, J.R. (1995) Cytochrome P450 and the metabolism of arachidonic acid and oxygenated eicosanoids in *Cytochrome P450: Structure, Mechanism and Biochemistry, 2nd edition* (Oritiz de Montellano, P.R., ed.) pp. 443–472, Plenum Press, New York and London
3. Sono, M., Roach, M.P., Coulter, E.D., and Dawson, J.H. (1996) Heme-containing oxygenases. *Chem. Rev.* **96**, 2841–2887
4. Poulos, T.L., Finzel, B.C., and Howard, A.J. (1986) Crystal structure of substrate-free *Pseudomonas putida* cytochrome P450. *Biochemistry* **25**, 5314–5322

Downloaded from http://jb.oxfordjournals.org/ at Peking University on October 1, 2012

5. Poulos, T.L., Finzel, B.C., and Howard, A.J. (1987) High-resolution crystal structure of cytochrome P450cam. *J. Mol. Biol.* **195**, 687–700
6. Raag, R. and Poulos, T.L. (1989) Crystal structure of the carbon monoxide-substrate-cytochrome P450cam ternary complex. *Biochemistry* **28**, 7586–7592
7. Benson, D.E., Berendzen, J., Chu, K., Stock, A.M., Maves, S.A., Benson, D., Sweet, R.M., Ringe, D., Petsko, G.A., and Sligar, S.G. (2000) The catalytic pathway of cytochrome P450cam at atomic resolution. *Science* **287**, 1615–1622
8. Raag, R., Martinis, S.A., Sligar, S.G., and Poulos, T.L. (1991) Crystal structure of the cytochrome P450cam active site mutant Thr252Ala. *Biochemistry* **30**, 11420–11429
9. Vidakovic, M., Sliger, S.G., Li, H., and Poulos, T.L. (1998) Understanding the role of the essential Asp251 in cytochrome p450cam using site-directed mutagenesis, crystallography, and kinetic solvent isotope effect. *Biochemistry* **37**, 9211–9219
10. Mueller, E.J., Loida, P.J., and Sligar, G.S. (1995) Twenty-five years of P450cam research in *Cytochrome P450: Structure, Mechanism, and Biochemistry, 2nd edition* (Ortiz de Montellano, P.R., ed.) pp. 83–124, Plenum Press, New York and London
11. Shimada, H., Sligar, S.G., Yeom, H., and Ishimura, Y. (1997) Heme monooxygenase—A chemical mechanism for cytochrome P450 oxygen activation in *Oxygenases and Model System* (Funabiki, T., ed.) Vol. 19, pp. 195–221, Kluwer Academic Publishers, Dordrecht/Boston/London
12. Katagiri, M., Ganguli, B.N., and Gunsalus, I.C. (1968) A soluble cytochrome P450 functional in methylene hydroxylation. *J. Biol. Chem.* **243**, 3543–3546
13. Ishimura, Y., Ullrich, V., and Peterson, J.A. (1971) Oxygenated cytochrome P-450 and its possible role in enzymic hydroxylation. *Biochem. Biophys. Res. Commun.* **42**, 140–146
14. Imai, M., Shimada, H., Watanabe, Y., Matsushima-Hibiya, Y., Makino, R., Koga, H., Horiuchi, T., and Ishimura, Y. (1989) Uncoupling of the cytochrome P-450cam monooxygenase reaction by a single mutation, threonine-252 to alanine or valine: A possible role of the hydroxy amino acid in oxygen activation. *Proc. Natl. Acad. Sci. USA* **86**, 7823–7827
15. Martinis, S.A., Atkins, W.M., Stayton, P.S., and Sligar, S.G. (1989) A conserved residue of cytochrome P450 is involved in heme-oxygen stability and activation. *J. Am. Chem. Soc.* **111**, 9252–9253
16. Gerber, N.C. and Sligar, S.G. (1992) Catalytic mechanism of cytochrome P450: Evidence for a distal charge relay. *J. Am. Chem. Soc.* **114**, 8742–8743
17. Kimata, Y., Shimada, H., Hirose, T., and Ishimura, Y. (1995) Role of Thr-252 in cytochrome P450cam: A study with unnatural amino acid mutagenesis. *Biochem. Biophys. Res. Commun.* **208**, 96–102
18. Shimada, H., Makino, R., Imai, M., Horiuchi, T., and Ishimura, Y. (1990) Mechanism of oxygen activation by cytochrome P-450-cam in *International Symposium on Oxygenases and Oxygen Activation* (Yamamoto, S., Nozaki, M., and Ishimura, Y., eds.) pp. 133–136, Yamada Science Foundation
19. Gunsalus, I.C. and Wagner, G.C. (1978) Bacterial P-450cam methylene monooxygenase components: Cytochrome *m*, putidaredoxin, and putidaredoxin reductase. *Methods Enzymol.* **52**, 166–188
20. Unno, M., Shimada, H., Toba, Y., Makino, R., and Ishimura, Y. (1996) Role of Arg^{112} of cytochrome P450cam in the electron transfer from reduced putidaredoxin. *J. Biol. Chem.* **271**, 17869–17874
21. Peterson, J.A. (1971) Camphor binding by *Pseudomonas putida* cytochrome P-450. *Arch. Biochem. Biophys.* **144**, 678–693
22. Griffin, B.W. and Peterson, J.A. (1972) Camphor binding by *Pseudomonas putida* cytochrome P450. Kinetics and thermodynamics of the reaction. *Biochemistry* **11**, 4740–4746
23. Hintz, M.J. and Peterson, J.A. (1980) The kinetics of reduction of cytochrome P-450cam by the dithinite anion monomer. *J. Biol. Chem.* **255**, 7317–7325
24. Davies, M.D. and Sligar, S.G. (1992) Genetic variants in the putidaredoxin-cytochrome P450cam electron-transfer complex: Identification of the residue responsible for redox-state-dependent conformers. *Biochemistry* **31**, 11383–11389
25. Brewer, C.B. and Peterson, J.A. (1988) Single turnover kinetics of the reaction between oxycytochrome P450cam and reduced putidaredoxin. *J. Biol. Chem.* **263**, 791–798
26. Poulos, T.L., Perez, M., and Wagner, G.C. (1982) Preliminary crystallographic data on cytochrome P450cam. *J. Biol. Chem.* **257**, 10427–10429
27. Adachi, S., Oguchi, T., and Ueki, T. (1996) Present status of RIKEN beamline II for structural biology (BL44B2). *Spring-8 Annual Report 1996*, 239–240
28. Leslie, A.G.W. (1994) MOSFILM users guide, MRC-LMB, Cambridge, UK
29. 4, C.c.p.n. (1994) The *CCP*4 suite: Programs for protein crystallography. *Acta Cryst.* **D50**, 760–763
30. Roussel, A. and Cambillau, C. (1989) *Silicon Graphics Geometry Partner Directory*, 77–78
31. Laskowski, R.A., MacArthur, M.W., Moss, D.S., and Thornton, J.M. (1993) PROCHECK: a program to check the stereochemical quality of protein structures. *J. Appl. Cryst.* **26**, 283–291
32. Hintz, M.J. and Peterson, J.A. (1981) The kinetics of reduction of cytochrome P-450cam by reduced putidaredoxin. *J. Biol. Chem.* **256**, 6721–6728
33. Unno, M., Christian, J.F., Benson, D.E., Gerber, N.C., Sligar, S.G., and Champion, P.M. (1997) Resonance raman investigations of cytochrome P450cam complexed with putidaredoxin. *J. Am. Chem. Soc.* **119**, 6614–6620
34. Aikens, J. and Sligar, S.G. (1994) Kinetic solvent isotope effects during oxygen activation by cytochrome P450cam. *J. Am. Chem. Soc.* **116**, 1143–1144
35. Gerber, N.C. and Sligar, S.G. (1994) A role of Asp-251 in cytochrome P-450cam oxygen activation. *J. Biol. Chem.* **269**, 4260–4266
36. Shimada, H., Makino, R., Unno, M., Horiuchi, T., and Ishimura, Y. (1993) Proton and electron transfer mechanism in dioxygen activation by cytochrome P450cam in *Cytochrome P450: Biochemistry, Biophysics and Molecular Biology* (Lechner, M.C., ed.) pp. 299–306, John Libbey Eurotext, Paris
37. Fukuzumi, S. (2000) Fundamental concepts of catalysis in electron transfer in *Electron Transfer in Chemistry* (Balzani, V., ed.) Vol. 5, Wiley-VCH, Weinheim, in press
38. Springer, B.A., Sligar, S.G., Olson, J.S., and Phillips, G.N., Jr. (1994) Mechanisms of ligand recognition in myoglobin. *Chem. Rev.* **94**, 699–714
39. Brantley, R.E.J., Smerdon, S.J., Wilkinson, A.J., Singleton, E.W., and Olson, J.S. (1993) The mechanism of autooxidation of myoglobin. *J. Biol. Chem.* **268**, 6995–7010

Downloaded from http://jb.oxfordjournals.org/ at Peking University on October 1, 2012